# Arctic Tropospheric Warming: Causes and Linkages to Lower Latitudes

JUDITH PERLWITZ

*Cooperative Institute for Research in Environmental Sciences, University of Colorado Boulder, and Physical Sciences Division, NOAA/Earth System Research Laboratory, Boulder, Colorado*

MARTIN HOERLING AND RANDALL DOLE

*Physical Sciences Division, NOAA/Earth System Research Laboratory, Boulder, Colorado*

ABSTRACT

Arctic temperatures have risen dramatically relative to those of lower latitudes in recent decades, with a common supposition being that sea ice declines are primarily responsible for amplified Arctic tropospheric warming. This conjecture is central to a hypothesis in which Arctic sea ice loss forms the beginning link of a causal chain that includes weaker westerlies in midlatitudes, more persistent and amplified midlatitude waves, and more extreme weather. Through model experimentation, the first step in this chain is examined by quantifying contributions of various physical factors to October–December (OND) mean Arctic tropospheric warming since 1979. The results indicate that the main factors responsible for Arctic tropospheric warming are recent decadal fluctuations and long-term changes in sea surface temperatures (SSTs), both located outside the Arctic. Arctic sea ice decline is the largest contributor to near-surface Arctic temperature increases, but it accounts for only about 20% of the magnitude of 1000–500-hPa warming. These findings thus disconfirm the hypothesis that deep tropospheric warming in the Arctic during OND has resulted substantially from sea ice loss. Contributions of the same factors to recent midlatitude climate trends are then examined. It is found that pronounced circulation changes over the North Atlantic and North Pacific result mainly from recent decadal ocean fluctuations and internal atmospheric variability, while the effects of sea ice declines are very small. Therefore, a hypothesized causal chain of hemisphere-wide connections originating from Arctic sea ice loss is not supported.

## 1. Introduction

During recent decades, temperature increases have been larger over the Arctic than over the rest of the globe, especially at the earth's surface but also in the troposphere (e.g., Lawrence et al. 2008; Graversen et al. 2008; Serreze et al. 2009; Bekryaev et al. 2010; Screen and Simmonds 2010; Screen et al. 2012). The observed enhanced warming of the Arctic, referred to as Arctic amplification (AA), has been most pronounced during fall and early winter (Screen et al. 2012, 2013b). The period of AA has generally coincided with accelerated Arctic sea ice loss, especially after 2000 (Stroeve et al. 2007; Comiso et al. 2008; Kumar et al. 2010; Parkinson

and Comiso 2013). These empirical and modeling studies indicate that the depletion of Arctic sea ice has been the dominant cause of observed Arctic surface warming.

In contrast, the explanation for observed Arctic tropospheric warming is a matter of controversy (e.g., Jeffries et al. 2013; Cohen et al. 2014; Walsh 2014). It has been conjectured that the magnitude of the Arctic warming throughout the lower-to-middle troposphere, as manifested by widespread increases in the 1000–500-hPa layer thickness, has been mainly an atmospheric response to Arctic sea ice loss (Francis and Vavrus 2012). However, numerical experiments using atmospheric models in which the observed changes in Arctic sea ice are specified find that the effects of sea ice loss on Arctic temperatures are primarily confined to the lowermost troposphere (e.g., Kumar et al. 2010; Screen et al. 2012, 2013a,b). These modeling studies suggest that Arctic amplification of warming through the lower-to-middle troposphere is unlikely to be due primarily to

sea ice loss. Alternate explanations for the observed warming aloft in the Arctic include increased poleward heat transport related to SST changes that have occurred outside the Arctic (Bitz and Fu 2008; Chung and Räisänen 2011; Laliberté and Kushner 2013; Screen et al. 2012; Ding et al. 2014). It is not known, however, whether the AA of deep tropospheric warming as observed in recent decades is primarily due to forcing of the atmosphere either locally or remotely, or if it may also involve an expression of atmospheric variability unrelated to lower boundary forcing.

The primary goal of this study is to quantify the magnitude of Arctic warming resulting from these aforementioned factors. By utilizing atmospheric general circulation models forced by specified changes in lower boundary conditions (SSTs and sea ice) as well as by atmospheric composition changes, we ask the following questions. What is the magnitude of Arctic deep tropospheric warming resulting from atmospheric sensitivity to observed Arctic sea ice loss? What is the magnitude of Arctic deep tropospheric warming resulting from atmospheric sensitivity to SST variations outside the polar cap? And what was the likely contribution to the warming by internal atmospheric variability alone?

The question on why the Arctic troposphere has warmed is important for interpreting how Arctic changes may be linked to lower-latitude weather variability. How sea ice loss affects the vertical structure of tropospheric temperature change over the Arctic is of particular interest because its characteristics bear critically on determining the efficacy of remote sea ice impacts on lower latitudes. That Arctic sea ice loss may have led to major changes in midlatitude weather and climate has been conjectured based primarily upon results from several empirical studies (Overland and Wang 2010; Francis and Vavrus 2012; Tang et al. 2013). The proposed mechanism that has received most attention to date starts by assuming that Arctic sea ice loss has been a primary driver of Arctic 1000–500-hPa thickness increases, especially during October–December. A smaller meridional thickness gradient between polar and midlatitudes implies a weaker upper-level westerly jet, which is hypothesized to slow the eastward progression and increase the meridional extent of midlatitude Rossby waves, producing more persistent and extreme weather conditions (Francis and Vavrus 2012). The proposition that sea ice loss leads to significant changes in midlatitude variability therefore rests fundamentally on evidence for the importance of sea ice contributions to driving observed Arctic tropospheric thickness changes.

Here, by assessing the causes for Arctic tropospheric warming, we also address the specific question of the strength of this critical first link in the chain proposed to connect sea ice depletion to midlatitude weather extremes. In this study, our principal focus will be on identifying causes for observed changes in Arctic tropospheric temperatures between the two decades 1979–88 and 2003–12 during October–December (OND), a period and time of year when the impact of recent Arctic sea ice loss on the atmosphere is likely to be maximized (e.g., Serreze et al. 2009; Screen et al. 2012, 2013b). Section 2 outlines the utilized reanalysis datasets, model experiments, and diagnostic methods. The results are described in section 3 and summarized and discussed in section 4.

## 2. Reanalysis datasets, model experiments, and diagnostic methods

Observed changes in atmospheric fields are estimated from four reanalysis datasets: NCEP–NCAR (Kalnay et al. 1996), NCEP–DOE AMIP-II (Kanamitsu et al. 2002), ERA-Interim (Dee et al. 2011), and JRA-25/ JMA Climate Data Assimilation System (JCDAS) (Onogi et al. 2007). Monthly gridded values for 1000–500-hPa thickness, tropospheric air temperatures and geopotential height, and 500-hPa zonal wind are available for each dataset from January 1979 through December 2012. The Twentieth-Century Reanalysis (20CR) (Compo et al. 2011) from 1901 to 2000 is also employed to estimate observed magnitudes of decadal variability.

Climate simulations are based on two atmospheric models: CAM4 (Neale et al. 2013) run at 0.94° latitude × 1.25° longitude resolution with 18 vertical levels in the troposphere, and ECHAM5 (Roeckner et al. 2003) run at spectral T156 (~0.75°) resolution with 25 vertical levels in the troposphere. Table 1 gives an overview of all experiments. In brief, fully forced experiments (AMIP) impose specified observed monthly varying sea surface temperatures (SSTs), sea ice concentrations (SICs), and greenhouse gas concentrations from January 1979 to December 2012. Ensemble-mean fields derived from the AMIP runs provide an estimate of the forced atmospheric response to the specific SSTs, SICs, and greenhouse gas concentrations that occurred over this period. A second set of runs has SSTs and greenhouse gas concentrations identical to the full AMIP runs but replaces the observed SIC with a repeating climatological seasonal cycle of SIC for 1979–88 (AMIP-noSIC). In the AMIP-noSIC runs, each grid box that is partially covered by sea ice has SSTs set to the 1979–88 climatological values [see Screen et al. (2013b) for a detailed discussion of this approach]. The atmospheric response attributable to forcing solely from Arctic sea ice changes between 1979–88 and 2003–12 is then estimated from the 2003–12 ensemble-mean differences

TABLE 1. Overview of model experiments.

| Experiment | SST | SIC | Radiative forcing | No. of runs/length of integration | |
|---|---|---|---|---|---|
| | | | | CAM4 | ECHAM5 |
| PI-Control | 1881–1910 climatology | 1881–1910 climatology | Preindustrial | 300 yr | 300 yr |
| PD-Control | 1981–2010 climatology | 1981–2010 climatology | 1981–2010 climatology | 300 yr | 300 yr |
| AMIP | 1979–2012 | 1979–2012 | 1979–2012 | 20 runs | 20 runs |
| AMIP-noSIC | 1979–2012 | 1979–89 climatology | 1979–2012 | 20 runs | 10 runs |

between the AMIP and the AMIP-noSIC runs. This approach is used to retain to the maximum extent the atmospheric responses to changes in components of the climate system other than sea ice during this period.

To estimate contributions to the decadal differences arising from long-term climate change, 300-yr-long preindustrial (PI-Control) and present-day control (PD-Control) simulations are performed. In these runs, prescribed monthly varying climatological SST, SIC, and radiative forcing (RF) are specified for the 30-yr periods 1881–1910 (PI-Control) and 1981–2010 (PD-Control) (see Table 1). Ensemble-mean differences between these two runs provide a basis for estimating contributions from long-term ocean surface temperature and radiative forcing changes to Arctic warming in recent decades (see appendix A for more details). Finally, the contribution to decadal atmospheric changes arising from decadal ocean variability is estimated from the difference between the ensemble-mean AMIP response and estimated contributions from long-term climate change and decadal sea ice changes, noting that almost all of the Arctic sea ice loss has occurred since 1979.

## 3. Results

### a. Decadal changes in SIC and SST

Figure 1 (top) shows that reduction of SIC in OND between decadal averages of 2003–12 versus 1979–88 covers most of the Arctic marginal seas, with maximum loss between 15°E and 150°W. Outside the Arctic, SSTs are also substantially different between these two periods (Fig. 1, middle). In particular, the North Atlantic exhibits widespread warming, whereas the Pacific Ocean is characterized by a horseshoe-shaped pattern of change with large warming in extratropical SSTs and relative cooling in the tropical eastern Pacific. The Northern Hemisphere pattern projects onto the negative phase of the Pacific decadal oscillation (PDO). The strong warming over the mid- and high-latitude North Atlantic is also consistent with a shift toward the positive phase of the Atlantic multidecadal oscillation (AMO).

Figure 1 (bottom) provides an estimate of the long-term change contribution to recent decadal differences in the geographical pattern (bottom left) and zonal-mean structure (bottom right) of SSTs based on the methods described in section 2 and appendix A. The long-term contribution to changes in SSTs between 1979–88 and 2003–12 consists of a relatively homogenous warming in most locations, with magnitudes typically between 0.2 and 0.6 K, especially in the North Atlantic south of 45°N and over the Indian Ocean. A comparison of the middle and bottom panels in Fig. 1 indicates that the pronounced regional warming between the two decades in the North Atlantic and large differences across much of the Pacific are likely related mostly to recent decadal ocean variability, rather than being a manifestation of long-term climate change.

We note that our observationally based estimate of the long-term SST change includes the impact of both anthropogenic (e.g., greenhouse gas increase and aerosols) and natural (volcanic eruptions and solar variability) climate forcings. Furthermore, our estimated recent decadal SST change may not be solely due to internal ocean variability but may also include a contribution of these climate forcings.

### b. Zonal-mean and Arctic perspective

Figure 2 compares reanalysis and climate model–simulated changes in OND zonal-mean temperature between the two decadal periods 2003–12 and 1979–88. The estimated zonal-mean temperature changes obtained from the average of the four reanalyses (top) show strong near-surface warming in the Arctic that exceeds four standard deviations (SDs) of observed decadal variability, as estimated through methods described in appendix B. Arctic warming is evident to the upper troposphere, with maximum increases below 850 hPa. The latitude–height structure of warming is consistent with results obtained in previous studies that focused on slightly different periods or months (e.g., Kumar et al. 2010; Serreze et al. 2009; Screen et al. 2013b). While various reanalysis products differ in the magnitude of warming over the Arctic (e.g., Bitz and Fu 2008;
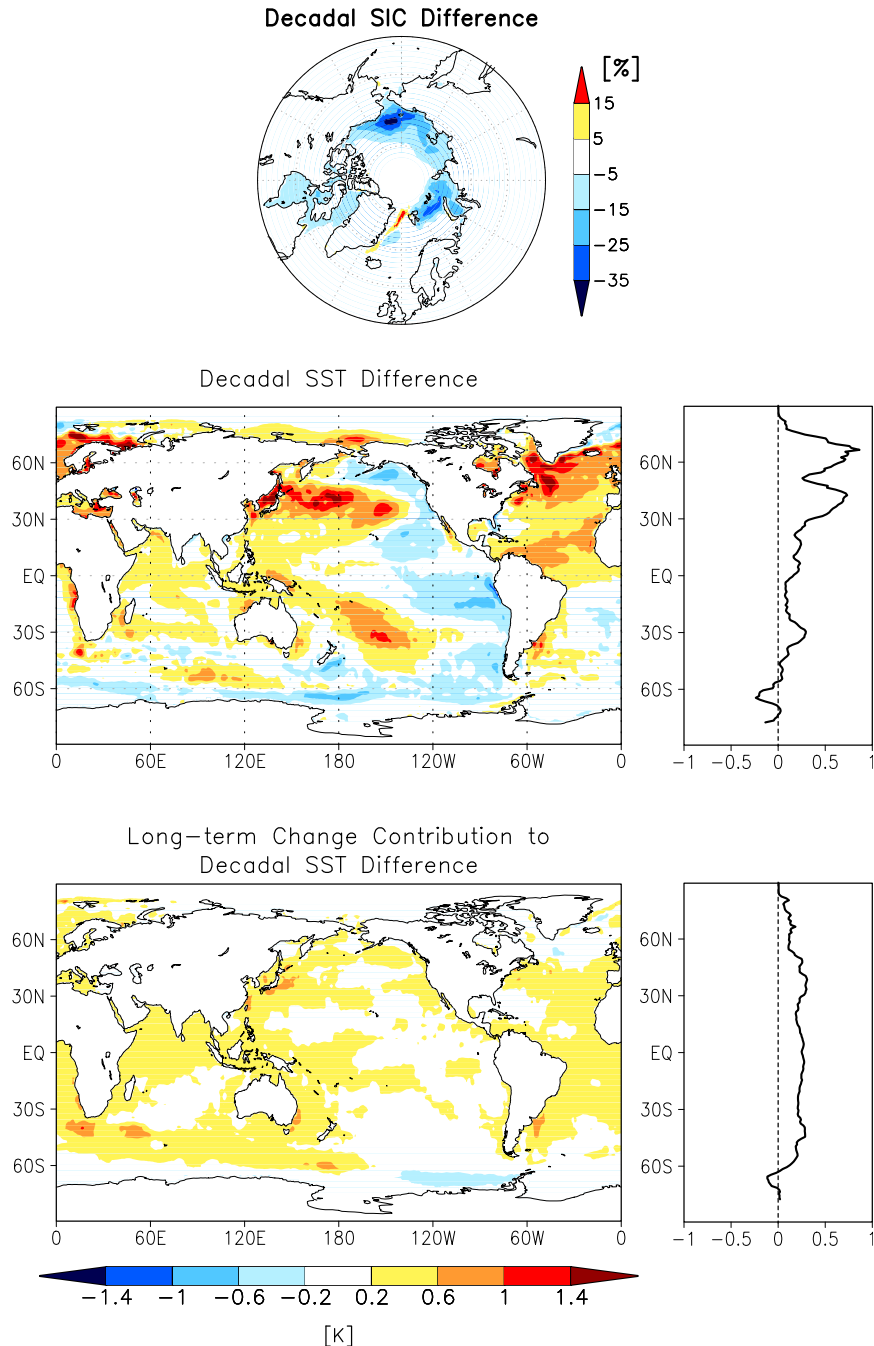
FIG. 1. Decadal difference (2003–12 minus 1979–88) of OND average for (top) SIC, (middle left) map and (middle right) zonal-mean total change of SST, and (bottom left) map and (bottom right) zonal-mean of long-term change contribution to decadal SST difference (see text in section 2c and appendix A for details). SST and SIC are taken from Hurrell et al. (2008).

Grant et al. 2008; Thorne 2008; Screen et al. 2012), this general latitude–height structure is robust to analysis uncertainty (not shown).

The tropospheric warming between the two decades is strongly forced by lower boundary changes and prescribed variations in radiative forcings, as indicated by the results of the AMIP simulations with the CAM4 and ECHAM5 (Fig. 2, middle left and middle right). The general pattern of the zonal-mean response is robust between the two different models. Consistent
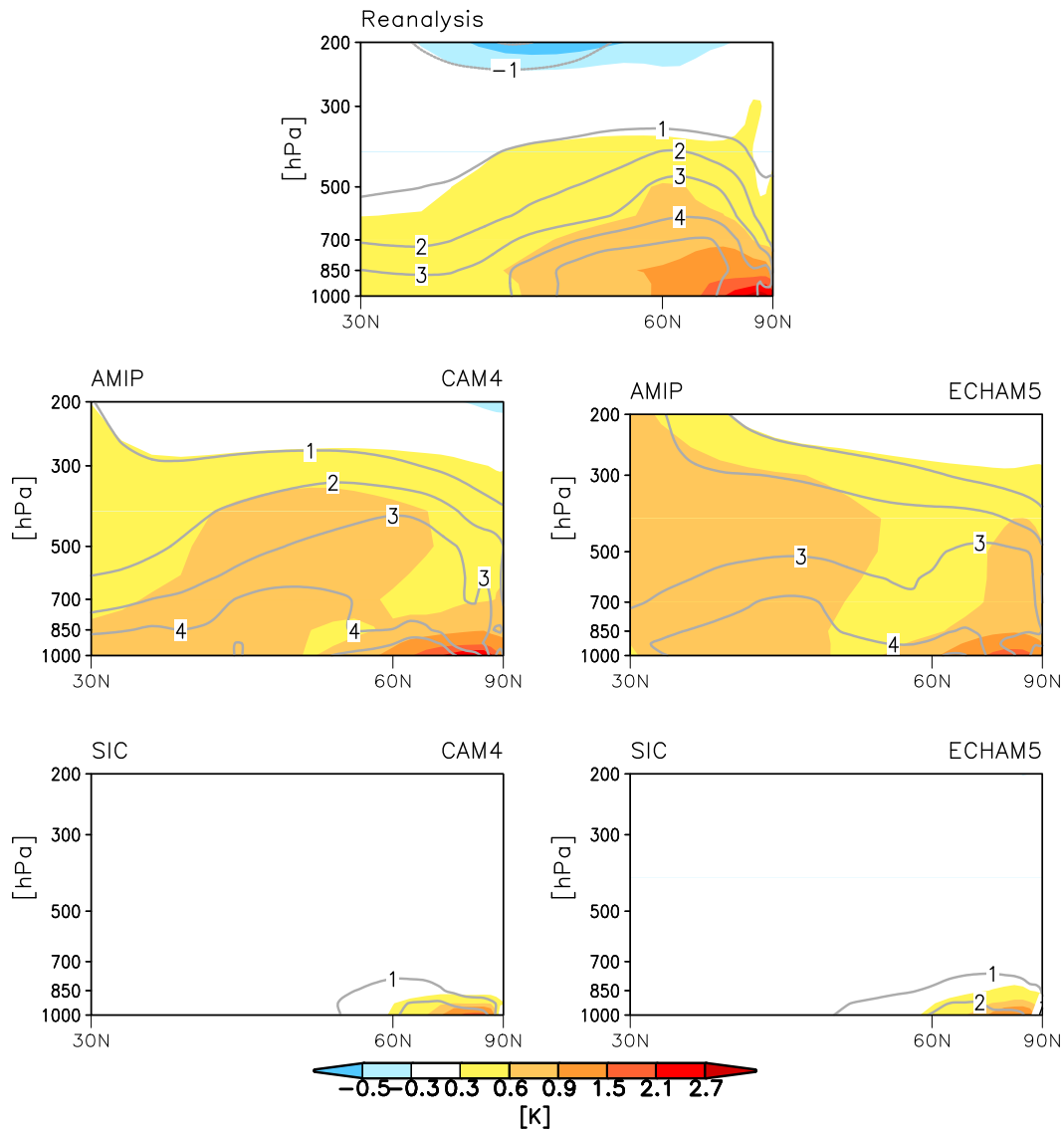
FIG. 2. Latitude–height cross sections of decadal zonal-mean temperature difference (2003–12 minus 1979–88) for OND of (top) average of four reanalyses, (middle) simulated zonal-mean temperature difference based on observed SST and radiative forcing (from AMIP) for (left) CAM4 and (right) ECHAM5, and (bottom) simulated 2003–12 mean contribution of sea ice loss to atmospheric zonal-mean temperature difference for (left) CAM4 and (right) ECHAM5. Gray contours indicate normalized differences based on one SD of observed decadal variability (see appendix B for details). Nonlinear scaling of the *x* axes takes into account the area of the globe represented by the zonal mean.

with the observed changes, the model responses show widespread and deep tropospheric warming in middle and high latitudes, with the strongest warming near the surface across the Arctic. However, there are also differences between the observed and simulated changes. In contrast with the observed temperature changes, the models do not show a substantial decrease in the mid-tropospheric temperature gradient between lower and higher latitudes. This characteristic of the observed

difference between the two periods cannot be explained by a sensitivity to lower boundary changes and prescribed changes in atmospheric composition. As will be discussed subsequently, this result has important implications for understanding the nature of Arctic linkages with lower latitudes.

To illustrate the specific nature of temperature impacts resulting from sea ice changes, the ensemble-mean difference between the AMIP and AMIP-noSIC simulations
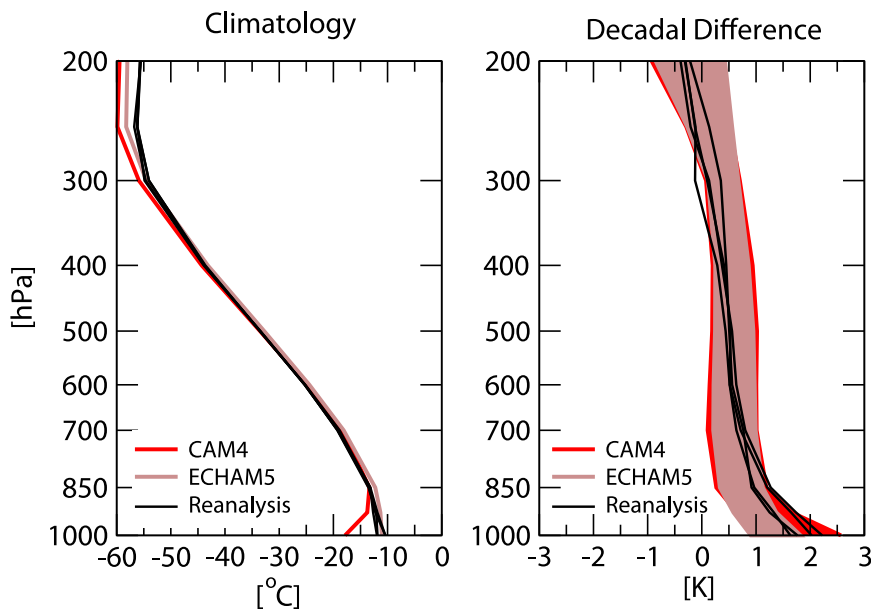
FIG. 3. Vertical profiles of polar cap (60°–90°N) temperature for OND of (left) 1979–2012 climatologies and (right) decadal differences (2003–12 minus 1979–88) for four reanalyses and AMIP ensemble means. Black lines indicate the four reanalysis profiles, and the red and brown indicate the CAM4 and ECHAM5, respectively, with shaded areas showing the range of simulated decadal differences (±2 SD).

for the period 2003–12 are shown in the bottom row of Fig. 2. Changes in zonal-mean temperatures resulting from sea ice loss alone are confined to the lowermost troposphere at high latitudes, a result consistent with several previous studies on the effect of sea ice loss on the Arctic atmosphere (e.g., Deser et al. 2010; Kumar et al. 2010; Screen et al. 2012, 2013a,b). The deep tropospheric Arctic warming and associated reduction in the midlatitude temperature gradients between the two periods seen in observations cannot be explained as responses to the sea ice changes, indicating that other mechanisms are needed to explain these features.

Figure 3 shows vertical profiles of OND temperatures spatially averaged over the polar cap (60°–90°N) for individual reanalyses and for the two models. The climatological profile (Fig. 3, left) is characterized by a strong surface-based inversion (being stronger in the CAM4 than in ECHAM5), with the inversion layer extending to approximately 850 hPa. The decadal differences in temperature (Fig. 3, right) are maximized below this inversion layer, with a somewhat weaker but near-constant warming occurring from just above the inversion layer to near the tropopause. The CAM4 shows greater surface warming than ECHAM5, consistent with the former's stronger surface-based inversion. Above this layer the temperature responses in the two models are in close agreement. All members of both models (the range of which is indicated by shading) are similar in

yielding a maximum in near-surface warming and a temperature rise throughout the entire depth of the troposphere. The range of model solutions resulting from internal decadal atmospheric variability is large compared to the spread among the four different reanalysis products, with the observational estimates falling within this range. The models are thus capable of producing decadal differences in the magnitude and vertical structure of Arctic warming similar to what has been observed.

To further illustrate the characteristics of climate trends since 1979, height changes on pressure surfaces from 1000 to 200 hPa are shown in Fig. 4. The heights of pressure surfaces have generally increased, as expected from the mass response to the observed tropospheric warming, with maximum increases in the upper troposphere as required from hydrostatic balance. Note, however, that at very high latitudes near the surface, the heights of pressure surfaces have declined. This feature is qualitatively consistent with the dynamical response expected to surface warming (Hoskins et al. 1985) and leads to smaller changes in the upper-level height fields than would be expected from consideration of thickness increases alone. In the upper troposphere, the meridional structure of decadal height differences consists of a broad maximum between 45° and 75°N (Fig. 4, top). This pattern describes a reduced meridional height gradient between lower and high latitudes, a condition
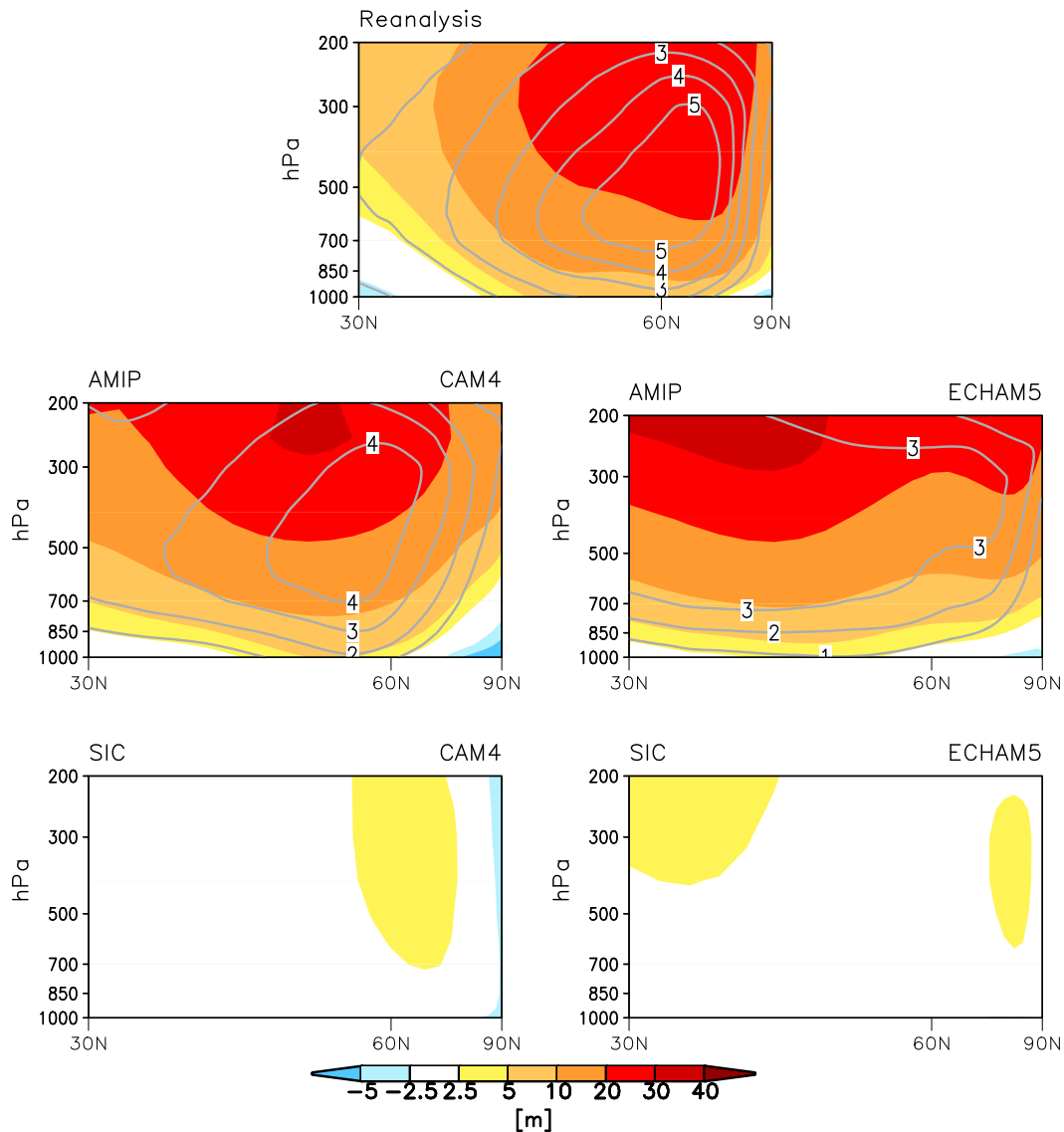
FIG. 4. As in Fig. 2, but for zonal-mean geopotential heights.

that is in geostrophic balance with weakened upper-tropospheric westerlies in middle latitudes.

The very large standardized departures for these high-latitude height changes (up to five standard deviations) implies that they are unlikely the result of internal atmospheric variability alone, an interpretation supported by the large magnitudes of ensemble-averaged anomalies occurring in both the CAM4 and ECHAM5 AMIP simulations (Fig. 4, middle). The model results indicate that many of the broad features of tropospheric height change represent sensitivity to lower boundary changes and prescribed changes in atmospheric composition, including the magnitude and the vertical profile of height changes. The near-surface height decreases over

the Arctic Ocean are also replicated in the models, but there are also notable differences from the observed decadal changes. In particular, neither model shows a substantial weakening in the midlatitude meridional height gradient in response to forcing. As found earlier, the large upper-level height rises also do not appear to be caused by sea ice changes between the two periods, with the amplitude of height differences resulting from sea ice changes alone being nearly an order of magnitude less than those in the fully forced AMIP simulations.

To further characterize recent Arctic warming and analyze contributing factors to the observed changes, probability distribution functions (PDFs) of simulated 1000–500-hPa thickness changes over the polar cap
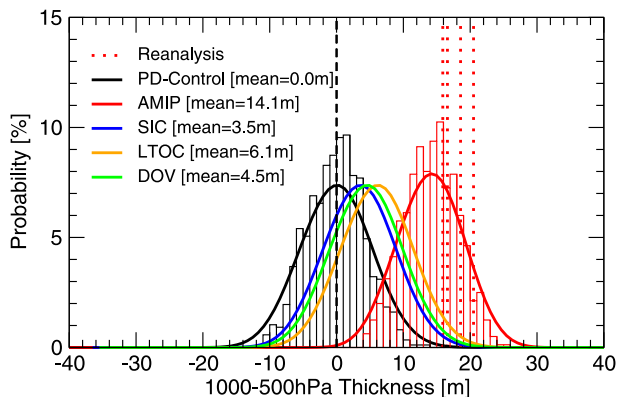
FIG. 5. Histograms and PDFs of OND decadal differences of polar cap (60°–90°N) 1000–500-hPa thickness for the 300-yr PD-Control run (black) and AMIP simulations (red; 2003–12 minus 1979–88) together with PDFs of estimated contributions of various factors to the fully forced AMIP thickness difference: SIC (blue), scaled LTOC (orange), and recent DOV (green). The histograms are based on the large ensemble approach described in appendix C. The shape of the PDFs is estimated from a nonparametric fit to the large sample histogram. The one SD of the large ensembles amounts to 4 m. We assume that the PDFs of the forced SIC, LTOC, and DOV signal are as in the PDF of the PD-Control run. The red dashed vertical lines indicate the decadal differences (2003–12 minus 1979–88) for the four reanalyses.

(60°–90°N) for OND are presented in Fig. 5. The PDFs are derived from a large ensemble of decadal differences determined between individual model runs through methods described in appendix C. The widths of these distributions provide estimates of the magnitudes of changes that might arise solely from internal atmospheric variability on decadal time scales. Figure 5 shows the statistical distribution of decadal differences in the AMIP experiments (red curve), together with four reanalysis estimates (dotted red lines), as well as a PDF of decadal differences determined from the 300-yr PD-Control run that has no changes in ocean or external radiative forcings (black curve). The one standard deviation of decadal differences in internal atmospheric decadal variability in 1000–500-hPa thickness as estimated from the unforced model experiment is about 4 m. Reanalysis estimates of thickness increases range from 16 to 20 m (a 20-m increase in 1000–500-hPa thickness corresponds to a +1-K change in layer-averaged temperature). All reanalysis estimates reside on the very extreme tail of the statistical distribution of decadal changes arising from internal atmospheric variability (black curve), indicating again that the observed thickness increase over the polar cap between the two decades is extremely unlikely to be explained by internal atmospheric variability alone.

In contrast, the observed thickness increase over the polar cap falls well within the distributions of decadal

differences estimated from the AMIP simulations, indicating the strong forced component. The observational estimates are all above the estimated model ensemble-mean thickness change of 14.1 m. While model deficiencies could account for the slightly smaller ensemble-mean AMIP thickness increase compared to observations, the larger observed changes could also be accounted for by the superposed effect of the forced component and one standard deviation (4 m) of variability arising from random internal atmospheric variations.

Figure 5 also shows PDFs of polar cap 1000–500-hPa thickness change due to specific lower boundary forcings. The effects of three factors are assessed: 1) Arctic sea ice loss (SIC; blue curve), 2) contribution of long-term ocean change outside the polar cap (LTOC; orange curve), and 3) recent decadal ocean variability (DOV; green curve). The effect of sea ice loss alone, as estimated in Fig. 2, contributes to a mean thickness increase of 3.5 m, corresponding to column warming of about 0.18 K (blue curve). This relatively small contribution is consistent with the limited vertical extent of sea ice warming (see Figs. 2 and 4) and is comparable to decadal differences that might be expected from internal atmospheric variability. Arctic warming resulting from climate change influences (especially long-term warming of SSTs) from outside the Arctic is estimated to be a somewhat larger contributing factor at 6.1 m, corresponding to column mean warming of about 0.32 K (orange curve).

We estimated a magnitude of 4.5 m to Arctic thickness changes between 1979–88 and 2003–12 from recent decadal ocean variations. This contribution is determined as the difference between the AMIP total forced change and sum of the sea ice and long-term climate change contributions, assuming no other significant forcings.

In summary, our modeling results indicate that deep tropospheric warming over the polar cap during recent decades was mainly a response to changes in lower boundary SSTs, sea ice, and atmospheric composition. Of the about 18-m observed increase in 1000–500-hPa thickness, we estimate that approximately 14 m resulted from the effects of such forcings of the atmosphere. Arctic sea ice loss was the principal factor driving Arctic surface warming but did not have a dominant effect in mean tropospheric warming. Modeling evidence indicates that the Arctic deep troposphere warmed primarily as a result of remote, rather than in situ, forcings since 1979, with the main drivers being recent decadal fluctuations in SSTs and a long-term climate change contribution of SSTs, both occurring outside the polar cap. Atmospheric internal decadal variability likely also contributed substantially to the total observed change,
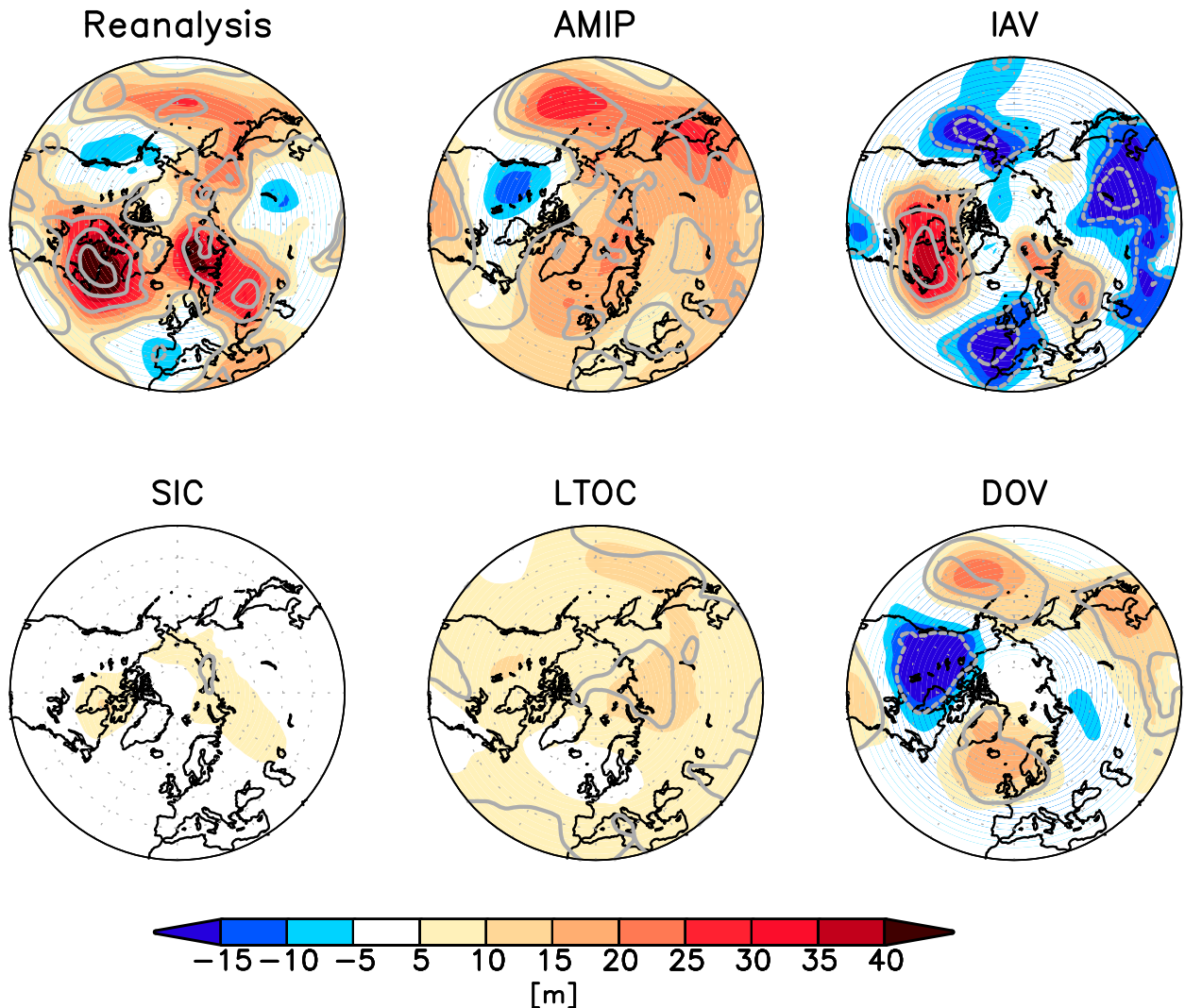
FIG. 6. Maps of decadal differences of 1000–500-hPa thickness for OND (2003–12 minus 1979–88). Shown are maps for the average of (top left) the four reanalyses, (top center) the fully forced experiment (from AMIP), (top right) internal atmospheric variability, (bottom left) contribution of Arctic sea ice loss, (bottom center) contribution of LTOC, and (bottom right) recent DOV. Map for simulated thickness changes are an average of the two model ensembles ECHAM5 and CAM4. Gray contours (−3, −2, −1, 1, 2, 3, and 4; negative values are dotted contours) indicate normalized differences based on one SD of observed decadal variability (see appendix B for details).

with a magnitude comparable to that of the sea ice loss effect.

### c. Regional perspective

While the "local effects" of sea ice change on polar cap–averaged tropospheric warming were found to be relatively small, could large-amplitude regional circulation anomalies in midlatitudes nonetheless have been a consequence of "remote effects" of Arctic sea ice change? To address this possibility, we have constructed spatial analyses of decadal OND 1000–500-hPa thickness differences derived from reanalysis and model

simulations (Fig. 6). Reanalysis differences between the two decades (Fig. 6, top left) include strong maxima over the North Atlantic southwest of Greenland and over the Barents Sea, and a wave train–like pattern emanating from low latitudes in the Pacific across North America. The AMIP signal (Fig. 6, top center) captures many of the observed features over the North Pacific. To the extent that this simulated signal is the true forced component that occurred in nature, the unforced internal atmospheric variability (IAV) contribution to decadal change can be inferred by differencing the observations and the AMIP ensemble mean. This estimated IAV

(Fig. 6, top right) exhibits large magnitude positive anomalies over the western North Atlantic that account for most of the observed decadal change in that region, with maximum values up to 2–3 SD of estimated observed decadal variability. That magnitudes this large could arise simply from random atmospheric variability is plausible insofar as they might be expected to occur by chance somewhere over the map area. Indeed, we found that individual members of the model ensemble simulated the magnitude of observed North Atlantic regional 1000–500-hPa thickness increase, though as a very extreme occurrence (not shown). Nonetheless, it is also possible that such a large magnitude for the inferred internal atmospheric variability in the North Atlantic may reflect limitations of the models or methods used to estimate the forced atmospheric response, and clarification will require analysis using additional models. In most other areas, however, the estimated magnitudes of IAV are on the order of one SD or less and are predominantly negative, suggesting this component might have contributed to a slight net tropospheric cooling between the two periods.

Figure 6 (bottom left) shows the contribution of sea ice loss to column thickness change. Its magnitude is much weaker than the effects of internal atmospheric variability over the midlatitudes, indicating a very low level of detectability of such a remote sea ice signal. The regional effects of sea ice loss are also weak compared to the effects of LTOC (Fig. 6, bottom center). The LTOC pattern is consistent with an overall global warming signature, with a relatively bland structure and weak spatial gradients in thickness.

The results provide evidence that the observed regional pattern of recent decadal thickness changes cannot be explained by influences from either Arctic sea ice loss or long-term ocean surface temperature changes. Instead, this pattern has been primarily a consequence of DOV. The spatial structure of the atmospheric impacts by DOV (Fig. 6, bottom right) exhibits a familiar wave train pattern arching from the tropical Pacific toward the North American continent that characterizes teleconnections associated with the cold phase of El Niño–Southern Oscillation. Physical considerations suggest that such a pattern would be expected given that the 1980s had multiple strong El Niño events, including the 1982–83 major event, while the 2000s have experienced more La Niña–like conditions. Indeed, this pattern is physically and dynamically consistent with the decadal differences of SSTs (Fig. 1, middle) that includes cold tropical eastern Pacific waters and a horseshoe of warm SSTs in the tropical western Pacific and North Pacific. Also apparent in the DOV-forced signal is a pronounced thickness increase over the eastern North

Atlantic, a feature identified in the model study by Ding et al. (2014) as well, although our estimated magnitude of the North Atlantic response appears weaker and shifted farther east.

The model results reveal a fundamental structural difference between the responses of tropospheric thickness to sea ice loss and/or long-term ocean temperature change and recent decadal ocean variability. The former is characterized by mostly uniform thickness increases and weak horizontal gradients, while the latter is characterized by wavelike patterns with strong horizontal gradients. Thus, despite the evidence that the combined contributions from sea ice loss and long-term SST change play a major role in explaining why the Arctic troposphere has warmed, dynamical effects of atmospheric wave structure linked to decadal ocean variability have been more important in explaining regional patterns of recent decadal OND change.

Such elemental differences in how various factors affect atmospheric circulation are clearly revealed by the responses of the midlatitude zonal flow. Figure 7 shows the observed features of decadal change consisting of a pronounced OND weakening of the westerlies over the North Atlantic region. The model evidence indicates this feature to have mainly resulted from a combination of internal atmospheric variability (Fig. 7, top right) and recent decadal ocean fluctuations (Fig. 7, bottom right). Contributions from forcing as a result of Arctic sea ice loss (Fig. 7, bottom left) and long-term SST change (Fig. 7, bottom center) are quite small, as is dynamically expected given that the thermal response to such forcings is quite uniform in space, thereby requiring little geostrophic adjustment of the winds.

Overall, these results indicate that the observed regional North America–North Atlantic decrease of midlatitude westerly zonal winds [e.g., as studied in Francis and Vavrus (2012) and Barnes (2013)] was neither a response to the remote effects of Arctic sea ice loss nor a signature of long-term SST change but was instead a reflection of the combined effects of internal atmospheric variability and decadal-scale ocean changes. Furthermore, the relatively weak sea ice signal compared to internal atmospheric noise or decadal SST-forced changes in dynamical properties like zonal wind makes it unlikely to be easily detectable on decadal time scales.

## 4. Summary and discussion

The context for this investigation on causes for Arctic tropospheric warming since 1979 is the open question on the role of Arctic sea ice loss in driving both Arctic and lower-latitude climate changes observed in recent decades. The notion of substantial effects rests critically on
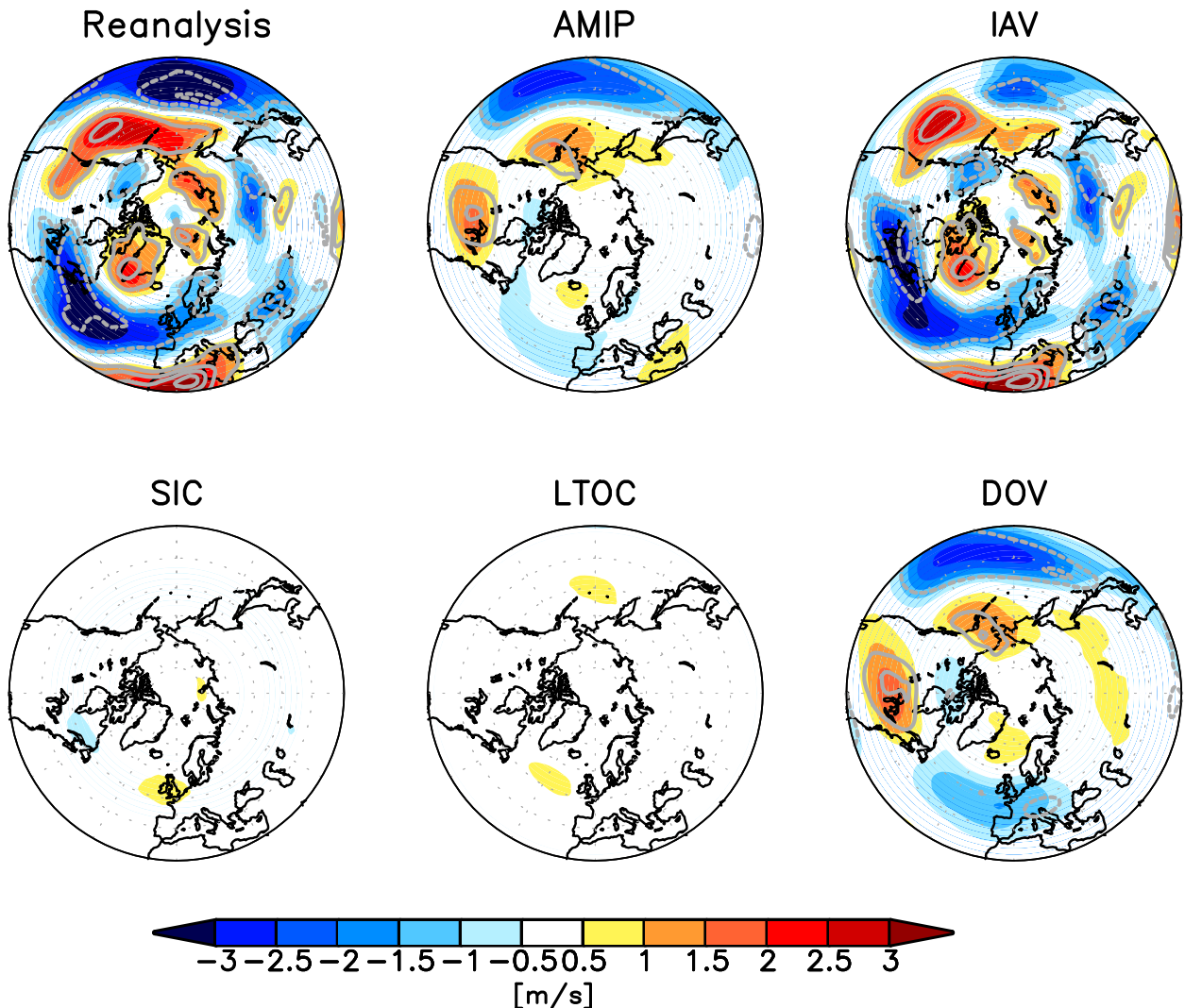
FIG. 7. As in Fig. 6, but for 500-hPa zonal wind.

the validity of the proposition that deep tropospheric warming in the Arctic has resulted from sea ice loss. Such warming has been speculated to set in motion a cascade of causal links tied to Arctic sea ice loss that include weaker upper-level westerlies in midlatitudes, more persistent and amplified midlatitude waves, and more extreme weather (Francis and Vavrus 2012). Our results from a suite of large ensemble multimodel simulations indicate that the magnitude of the observed Arctic tropospheric warming during OND cannot be reconciled with the effects of depleted Arctic sea ice. We found that only about 20% of observed Arctic averaged tropospheric thickness increase between 1979–88 and 2003–12 has resulted from sea ice loss alone. This relative small magnitude qualitatively agrees with the results of Screen et al. (2013a), who concluded that,

because of large internal atmospheric variability, sea ice contribution to tropospheric height increase over the Arctic during 1979–2009 was most likely not detectable. Our results further indicate the dominant drivers of observed Arctic tropospheric thickness increase are from SST changes that occurred outside of the polar cap. Recent decadal ocean variability and long-term ocean surface temperature changes were estimated to have contributed about 25% and 34%, respectively. Furthermore, the effect of internal atmospheric variability is shown to have substantially contributed to Arctic warming in recent decades, with a magnitude similar to the impact of sea ice loss alone.

The results of this study therefore disconfirm the hypothesis that deep tropospheric warming in the Arctic during recent decades and the OND season has resulted

substantially from sea ice loss. In this sense, the hypothesized chain of hemisphere-wide connections originating from Arctic sea ice loss is not supported, at least not in the simple linear framework proposed by Francis and Vavrus (2012). While finding that the "local effects" of sea ice change on polar cap–averaged tropospheric warming were relatively small, we nonetheless explored the possibility that observed large-amplitude regional circulation changes outside of the Arctic could have arisen from "remote effects" of Arctic sea ice change, perhaps via a hitherto unexplored nonlinear sensitivity of midlatitudes to Arctic sea ice loss. Model simulations and empirical analysis indicated that the observed midlatitude regional atmospheric circulation changes during recent decades were mainly due to a forced response to decadal ocean fluctuations and unforced internal atmospheric variability. The contributions of Arctic sea ice loss and long-term SST change outside the Arctic polar cap had little explanatory power for regional midlatitude circulation features, in particular, failing to explain the substantial weakening of the westerlies that was observed to occur over the North Atlantic during OND between the two decades.

There is general consistency between the results obtained from the two different models used in this study and findings from other modeling studies. Nevertheless, there are several sources of uncertainty and limitations of this study that should be noted. Among those factors are uncertainties in the prescribed radiative forcings and, especially, in estimating the long-term ocean surface temperature change contribution to recent observed decadal SST variations. We do not assess, nor do our methods permit, an evaluation of human-induced, natural externally forced or perhaps internal coupled ocean variability.

Other limiting factors are inherent in issues that arise when relying on climate models to draw inferences of cause and effect. Model studies to date have tended to find only weak impacts of sea ice loss on deep tropospheric temperatures, and, in this sense, our results are consistent with this prior body of evidence. However, studies have often been limited by small ensemble sizes for individual models and, in most instances, have not considered the statistical distributions of ensemble members. Similar to Screen at al. (2013a), we have examined the results from two different models and affirmed a strong reproducibility in results both for the thermal and dynamical responses. We have also used large ensemble methods, permitting quantitative diagnosis of larger statistical samples than in prior studies, from which we were able to examine variations in the nature of Arctic tropospheric warming in individual ensemble members. This presents a significant step forward in model-based approaches to understanding how the Arctic has warmed. The methods used herein have enabled us to estimate the inherent atmospheric noise contribution to recent Arctic climate change, which our results suggest may account for over 20% of the observed tropospheric 1000–500-hPa warming averaged over the polar cap between 1979–88 and 2003–12. An important limitation is that our model-based estimates of internal atmospheric variability are difficult to verify from observations. We would note, however, that the recent Fifth Assessment Report (AR5) of the Intergovernmental Panel on Climate Change (Stocker et al. 2013, p. 907) states, "Arctic temperature anomalies in the 1930s were apparently as large as those in the 1990s and 2000s. There is still considerable discussion of the ultimate causes of the warm temperature anomalies that occurred in the Arctic in the 1920s and 1930s." This observational evidence suggests that an important contribution to Arctic warming over periods of decades can originate from internal oceanic and atmospheric variations alone without requiring a strong external forcing.

An attribution study of the impacts of observed sea ice loss on atmospheric temperatures requires prescribing the observed sea ice conditions as boundary conditions within atmospheric circulation models. The possible limitations of such an approach were tested by comparing a parallel set of transient experiments with the coupled CCSM4 and atmosphere-only CAM4, with the latter prescribing the CCSM4 SIC and SST changes. Our results did not indicate a substantial impact of ocean coupling on the amount of Arctic deep tropospheric warming under current rates of sea ice loss (not shown).

Our study focused on the OND season, a period and time of year when the impact of recent Arctic sea ice loss on the atmosphere is likely to be maximized, as shown in several previous studies. Investigating the linkages between Arctic sea ice loss and the lower latitudes throughout the course of the seasonal cycle is a topic of future research.

## APPENDIX A

### Estimating Long-Term Climate Change Contributions to Recent Decadal Change

The contribution of long-term climate change to recent Arctic warming is estimated based on the PD-Control and PI-Control simulations. We first determine the difference between the PD-Control and PI-Control simulations and then scale this century-scale response relative to the recent period (change between 1979–88 and 2003–12). The scaling of the response is based on the relative change in observed global-mean (outside Arctic) surface temperature between the 1981–2010 mean and 1881–1910 mean period and the more recent 1979–88 and 2003–12 period. We determined a century-scale surface temperature change of 0.63 K and a recent temperature change of 0.33 K leading to a scaling factor of 0.52 of the recent change relative to the long-term response. Our scaling approach takes into account that both radiative forcing and global-mean temperature have not increased linearly over the last century (Fig. 8.18 in Myhre et al. 2013; Fig. 1a in Alexander et al. 2013). Utilizing the century-scale forced response also reduces the potential effects of internal multidecadal SST variability on our estimates of the climate change contribution.

## APPENDIX B

### Estimating Decadal Variability Based on the Twentieth-Century Reanalysis

We estimate the magnitude of observed decadal variability for zonal-mean temperature and geopotential height, 1000–500-hPa thickness, and 500-hPa zonal wind utilizing 20CR for the period 1901–2000 before the most rapid Arctic sea ice loss. In a first step, we remove the long-term linear trend. In a second step, we calculate 1-yr overlapping decadal averages. We then determine a large ensemble of nonoverlapping decadal differences between all decadal values. The one standard deviation derived from this ensemble is used as a measure of observed decadal variability of the atmosphere–ocean system.

## APPENDIX C

### Large Ensemble Approach

To better estimate the shape of PDFs for decadal differences the following large ensemble approach is used. For the 300-yr control runs, we determine the mean of 30 nonoverlapping decades and a subsequent ensemble of differences between all decadal values (total of 435). For the 20-member AMIP-style simulations, the large ensembles of decadal differences are created by differencing each of the 1979–88 averages with each of the 2003–12 averages of a particular model's member ensemble. Thus, the 20-member CAM4 and ECHAM5 AMIP simulations generate 400-member ensembles of decadal differences. We have verified that there is no statistical correlation between decadal averages, aside from that occurring as a result of the effects of specified forcing. The CAM4 and ECHAM5 yield very similar results (not shown); thus, the models are combined, allowing the generation of ensembles with at least 800 members. The shape of the resulting PDFs is estimated from a nonparametric fit to the multimodel combined large samples.

### REFERENCES

Alexander, L. V., and Coauthors, 2013: Summary for policymakers. *Climate Change 2013: The Physical Science Basis.* T. F. Stocker et al., Eds., Cambridge University Press, 3–29. [Available online at http://www.climatechange2013.org/images/report/WG1AR5_SPM_FINAL.pdf.]

Barnes, E. A., 2013: Revisiting the evidence linking Arctic amplification to extreme weather in midlatitudes. *Geophys. Res. Lett.,* **40,** 4728–4733, doi:10.1002/grl.50880.

Bekryaev, R. V., I. V. Polyakov, and V. A. Alexeev, 2010: Role of polar amplification in long-term surface air temperature variations and modern Arctic warming. *J. Climate,* **23,** 3888–3906, doi:10.1175/2010JCLI3297.1.

Bitz, C. M., and Q. Fu, 2008: Arctic warming aloft is dataset dependent. *Nature,* **455,** E3–E4, doi:10.1038/nature07258.

Chung, C. E., and P. Räisänen, 2011: Origin of the Arctic warming in climate models. *Geophys. Res. Lett.,* **38,** L21704, doi:10.1029/2011GL049816.

Cohen, J., and Coauthors, 2014: Recent Arctic amplification and extreme mid-latitude weather. *Nat. Geosci.,* **7,** 627–637, doi:10.1038/ngeo2234.

Comiso, J. C., C. L. Parkinson, R. Gersten, and L. Stock, 2008: Accelerated decline in the Arctic sea ice cover. *Geophys. Res. Lett.,* **35,** L01703, doi:10.1029/2007GL031972.

Compo, G. P., and Coauthors, 2011: The Twentieth Century Reanalysis project. *Quart. J. Roy. Meteor. Soc.,* **137,** 1–28, doi:10.1002/qj.776.

Dee, D. P., and Coauthors, 2011: The ERA-Interim reanalysis: Configuration and performance of the data assimilation system. *Quart. J. Roy. Meteor. Soc.,* **137,** 553–597, doi:10.1002/qj.828.

Deser, C., R. Tomas, M. Alexander, and D. Lawrence, 2010: The seasonal atmospheric response to projected Arctic sea ice loss in the late twenty-first century. *J. Climate,* **23,** 333–351, doi:10.1175/2009JCLI3053.1.

Ding, Q., J. M. Wallace, D. S. Battisti, E. J. Steig, A. J. Gallant, H. Kim, and L. Geng, 2014: Tropical forcing of the recent rapid Arctic warming in northeastern Canada and Greenland. *Nature,* **509,** 209–212, doi:10.1038/nature13260.

Francis, J. A., and S. J. Vavrus, 2012: Evidence linking Arctic amplification to extreme weather in mid-latitudes. *Geophys. Res. Lett.,* **39,** L06801, doi:10.1029/2012GL051000.

Grant, A., S. Brönnimann, and L. Haimberger, 2008: Recent Arctic warming vertical structure contested. *Nature,* **455,** E2–E3, doi:10.1038/nature07257.

Graversen, R. G., T. Mauritsen, M. Tjernström, E. Källén, and G. Svensson, 2008: Vertical structure of recent Arctic warming. *Nature,* **451,** 53–56, doi:10.1038/nature06502.

Hoskins, B. J., M. E. McIntyre, and A. W. Robertson, 1985: On the use and significance of isentropic potential vorticity maps. *Quart. J. Roy. Meteor. Soc.,* **111,** 877–946, doi:10.1002/qj.49711147002.

Hurrell, J. W., J. J. Hack, D. Shea, J. M. Caron, and J. Rosinski, 2008: A new sea surface temperature and sea ice boundary data set for the Community Atmosphere Model. *J. Climate,* **21,** 5145–5153, doi:10.1175/2008JCLI2292.1.

Jeffries, M., J. E. Overland, and D. K. Perovich, 2013: The Arctic shifts to a new normal. *Phys. Today,* **66,** 35–40, doi:10.1063/PT.3.2147.

Kalnay, E., and Coauthors, 1996: The NCEP/NCAR 40-Year Reanalysis Project. *Bull. Amer. Meteor. Soc.,* **77,** 437–471, doi:10.1175/1520-0477(1996)077<0437:TNYRP>2.0.CO;2.

Kanamitsu, M., W. Ebisuzaki, J. Woollen, S.-K. Yang, J. J. Hnilo, M. Fiorino, and G. L. Potter, 2002: NCEP–DOE AMIP-II Reanalysis (R-2). *Bull. Amer. Meteor. Soc.,* **83,** 1631–1643, doi:10.1175/BAMS-83-11-1631.

Kumar, A., and Coauthors, 2010: Contribution of sea ice loss to Arctic amplification. *Geophys. Res. Lett.,* **37,** L21701, doi:10.1029/2010GL045022.

Laliberté, F., and P. J. Kushner, 2013: Isentropic constraints by midlatitude surface warming on the Arctic midtroposphere. *Geophys. Res. Lett.,* **40,** 606–611, doi:10.1029/2012GL054306.

Lawrence, D. M., A. G. Slater, R. A. Tomas, M. M. Holland, and C. Deser, 2008: Accelerated Arctic land warming and permafrost degradation during rapid sea ice loss. *Geophys. Res. Lett.,* **35,** L11506, doi:10.1029/2008GL033985.

Myhre, G., and Coauthors, 2013: Anthropogenic and natural radiative forcing. *Climate Change 2013: The Physical Science Basis.* T. F. Stocker, et al., Eds., Cambridge University Press, 661–684. [Available online at https://www.ipcc.ch/pdf/assessment-report/ar5/wg1/WG1AR5_Chapter08_FINAL.pdf.]

Neale, R. B., J. Richter, S. Park, P. H. Lauritzen, S. J. Vavrus, P. J. Rasch, and M. Zhang, 2013: The mean climate of the Community Atmosphere Model (CAM4) in forced SST and fully coupled experiments. *J. Climate,* **26,** 5150–5168, doi:10.1175/JCLI-D-12-00236.1.

Onogi, K., and Coauthors, 2007: The JRA-25 Reanalysis. *J. Meteor. Soc. Japan,* **85,** 369–432, doi:10.2151/jmsj.85.369.

Overland, J. E., and M. Wang, 2010: Large-scale atmospheric circulation changes are associated with the recent loss of Arctic sea ice. *Tellus,* **62A,** 1–9, doi:10.1111/j.1600-0870.2009.00421.x.

Parkinson, C. L., and J. C. Comiso, 2013: On the 2012 record low Arctic sea ice cover: Combined impact of preconditioning and an August storm. *Geophys. Res. Lett.,* **40,** 1356–1361, doi:10.1002/grl.50349.

Roeckner, E., and Coauthors, 2003: The atmospheric general circulation model ECHAM5. Part I: Model description. Max Planck Institute for Meteorology Tech. Rep. 349, 127 pp. [Available online at http://www.mpimet.mpg.de/fileadmin/publikationen/Reports/max_scirep_349.pdf.]

Screen, J. A., and I. Simmonds, 2010: The central role of diminishing sea ice in recent Arctic temperature amplification. *Nature,* **464,** 1334–1337, doi:10.1038/nature09051.

——, C. Deser, and I. Simmonds, 2012: Local and remote controls on observed Arctic warming. *Geophys. Res. Lett.,* **39,** L10709, doi:10.1029/2012GL051598.

——, ——, ——, and R. Tomas, 2013a: Atmospheric impacts of Arctic sea-ice loss, 1979–2009: Separating forced change from atmospheric internal variability. *Climate Dyn.,* **43,** 333–344, doi:10.1007/s00382-013-1830-9.

——, I. Simmonds, C. Deser, and R. Tomas, 2013b: The atmospheric response to three decades of observed Arctic sea ice loss. *J. Climate,* **26,** 1230–1248, doi:10.1175/JCLI-D-12-00063.1.

Serreze, M. C., A. P. Barrett, J. C. Stroeve, D. N. Kindig, and M. M. Holland, 2009: The emergence of surface-based Arctic amplification. *Cryosphere,* **3,** 11–19, doi:10.5194/tc-3-11-2009.

Stocker, T. F., and Coauthors, 2013: *Climate Change 2013: The Physical Science Basis.* Cambridge University Press, 1535 pp. [Available online at http://www.climatechange2013.org/images/report/WG1AR5_ALL_FINAL.pdf.]

Stroeve, J., M. M. Holland, W. Meir, T. Scambos, and M. Serreze, 2007: Arctic sea ice decline: Faster than forecast. *Geophys. Res. Lett.,* **34,** L09501, doi:10.1029/2007GL029703.

Tang, Q., X. Zhang, X. Yang, and J. A. Francis, 2013: Cold winter extremes in northern continents linked to Arctic sea ice loss. *Environ. Res. Lett.,* **8,** 014036, doi:10.1088/1748-9326/8/1/014036.

Thorne, P., 2008: Arctic tropospheric warming amplification? *Nature,* **455,** E1–E2, doi:10.1038/nature07256.

Walsh, J. E., 2014: Intensified warming of the Arctic: Causes and impacts on middle latitudes. *Global Planet. Change,* **117,** 52–63, doi:10.1016/j.gloplacha.2014.03.003.